Developmental Biology 365 (2012) 208–218

Contents lists available at SciVerse ScienceDirect

Developmental Biology

journal homepage: www.elsevier.com/developmentalbiology

Combinatorial use of translational co-factors for cell type-specific regulation during neuronal morphogenesis in *Drosophila*

Eugenia C. Olesnicky [a,b], Balpreet Bhogal [a], Elizabeth R. Gavis [a,*]

[a] Department of Molecular Biology, Princeton University, Princeton, NJ 08544, USA
[b] Department of Biology, University of Colorado at Colorado Springs, Colorado Springs, CO 80918, USA

ARTICLE INFO

Article history:
Received for publication 17 November 2011
Revised 15 February 2012
Accepted 20 February 2012
Available online 25 February 2012

Keywords:
Brain tumor
Nanos
Pumilio
Dendrite morphogenesis
Neuromuscular junction

ABSTRACT

The translational regulators Nanos (Nos) and Pumilio (Pum) work together to regulate the morphogenesis of dendritic arborization (da) neurons of the *Drosophila* larval peripheral nervous system. In contrast, Nos and Pum function in opposition to one another in the neuromuscular junction to regulate the morphogenesis and the electrophysiological properties of synaptic boutons. Neither the cellular functions of Nos and Pum nor their regulatory targets in neuronal morphogenesis are known. Here we show that Nos and Pum are required to maintain the dendritic complexity of da neurons during larval growth by promoting the outgrowth of new dendritic branches and the stabilization of existing dendritic branches, in part by regulating the expression of *cut* and *head involution defective*. Through an RNA interference screen we uncover a role for the translational co-factor Brain Tumor (Brat) in dendrite morphogenesis of da neurons and demonstrate that Nos, Pum, and Brat interact genetically to regulate dendrite morphogenesis. In the neuromuscular junction, Brat function is most likely specific for Pum in the presynaptic regulation of bouton morphogenesis. Our results reveal how the combinatorial use of co-regulators like Nos, Pum and Brat can diversify their roles in post-transcriptional regulation of gene expression for neuronal morphogenesis.

Introduction

Neurons are highly polarized cells whose dendritic and axonal processes adopt distinct morphologies necessary for reception and transmission of signals. For example, the specific arborization patterns of dendrites in different types of sensory neurons are essential for neurons to establish their receptive fields and to respond to appropriate signals. At the neuromuscular junction (NMJ), axons must form specialized synaptic structures called boutons to regulate muscle dynamics. Post-transcriptional regulatory mechanisms including mRNA splicing, mRNA transport, and local control of protein synthesis have been implicated in the development of such polarized morphologies (Baines, 2005; Wu et al., 2007) and mutations in RNA-binding proteins involved in these processes have been linked to neuronal morphology defects associated with neurodegenerative and mental retardation disorders (Bassell and Warren, 2008; Fallini et al., 2011).

The dendritic arborization (da) neurons in the *Drosophila* larval peripheral nervous system (PNS) have provided a model for studying mechanisms underlying dendrite morphogenesis, including post-transcriptional control. These neurons are divided into four classes based on the complexity of their dendritic arbors, with class IV neurons exhibiting the most highly complex branching patterns. During late embryogenesis and early larval development, class IV da neurons elaborate their dendrites in a non-overlapping manner to establish large receptive fields that cover the larval body wall. Subsequently, as the larva increases dramatically in size, dendrites grow in synchrony with the body wall epithelium to maintain receptive field coverage (Parrish et al., 2009). Finally, class IV da neuron dendrites are pruned during pupariation in a process involving branch severing and caspase-mediated degeneration and are replaced by dendrites appropriate for the adult nervous system (Williams and Truman, 2005a; Williams and Truman, 2005b).

Mutations in the evolutionarily conserved translational repressors Nanos (Nos) and Pumilio (Pum) result in reduced higher order dendritic branching and dendritic field coverage in class IV da neurons (Brechbiel and Gavis, 2008; Ye et al., 2004). Nos and Pum were first identified as components of a translational repression complex that regulates embryonic patterning (Parisi and Lin, 2000), and genetic analysis indicates that they also act collaboratively in class IV da neurons (Ye et al., 2004). Moreover, dendritic localization of *nos* mRNA is required for dendrite branching morphogenesis (Brechbiel and Gavis, 2008), suggesting that Nos and Pum might mediate local control of translation.

Pum binds specifically to a sequence termed the Nanos Response Element (NRE) in the 3′ untranslated region (3′UTR) of target mRNAs. In a paradigm derived from analysis of Nos/Pum-dependent regulation of *hunchback* (*hb*) mRNA in the early embryo, Pum recruits Nos to the NRE to form a ternary complex, to which a third protein, Brain tumor

* Corresponding author.
E-mail address: gavis@princeton.edu (E.R. Gavis).

0012-1606/$ – see front matter © 2012 Elsevier Inc. All rights reserved.
doi:10.1016/j.ydbio.2012.02.028

(Brat) is then recruited to form a functional repression complex (Muraro et al., 2008; Sonoda and Wharton, 2001). Regulation of some targets by the Nos/Pum complex, however, does not require Brat (Harris et al., 2011; Muraro et al., 2008). Moreover, Nos and Pum can act independently and even in opposition to one another. In the ovary, Pum functions independently of Nos, but together with Brat to promote germline stem cell differentiation (Harris et al., 2011). In the NMJ, Nos and Pum have opposing functions in regulating both bouton formation and glutamate receptor subunit composition, thereby differentially regulating NMJ physiology (Menon et al., 2009). Thus, Nos, Pum, and Brat participate combinatorially in distinct complexes that act on different targets. Whether Brat is required by Nos and/or Pum in da neurons and in the NMJ is unknown.

To better understand the role of translational control in neuronal morphogenesis, we investigated the specific functions of Nos and Pum in dendrite elaboration by sensory neurons. Live imaging analysis revealed that Nos and Pum are required to maintain dendritic complexity during the third larval instar by promoting the addition of new branches and the stabilization of existing branches. We show that Nos and Pum control dendritic branching in part by repressing the expression of the pro-apoptotic factor Head Involution Defective (Hid). In addition, Nos and Pum exert differential effects on the level of the transcription factor Cut, indicating distinct target-specific requirements for these translational repressors. Finally, we uncover a role for Brat in the development of class IV da neurons and show that Brat functions together with Nos and Pum in dendrite morphogenesis. In contrast, Brat functions similarly to Pum and in opposition to Nos to regulate bouton morphogenesis in the NMJ. Our results show how control of gene expression during development can be diversified through the combinatorial use of translational co-regulators to generate distinct neuronal morphologies and, potentially, functions.

Materials and methods

Fly strains

The following fly strains were used: *GAL4^{477}*, *UAS-mCD8:GFP* (Grueber et al., 2003); *ppk-GAL4*, *UAS-mCD8:GFP* (Grueber et al., 2007), *OK6-GAL4*, *UAS-syt:GFP* (Aberle et al., 2002); *Mef2-GAL4* (Ranganayakulu et al., 1996); *MHC82-Gal4* (Marek et al., 2000); *UAS-nosRNAi* (Menon et al., 2009); *UAS-bratRNAi^{VDRC}* (*P{KK113206}*; Dietzl et al., 2007); *UAS-bratRNAi^{TRIP}* (*P{TRiP.HMS01121}*; Transgenic RNAi Project, Harvard Medical School); *UAS-brat* (Sonoda and Wharton, 2001); *UAS-bratRD* (Harris et al., 2011); *UAS-nos-tub3′UTR* (Clark et al., 2002); *UAS-pum* (Ye et al., 2004); *dlg::YFP* (Rees et al., 2011); *Df(3 L) H99* (Abbott and Lengyel, 1991); *ct^{c145}* (Grueber et al., 2003); and *d4EHP^{CP53}* (Cho et al., 2006). Larvae mutant for *nos* were generated by using the strong hypomorphic combination *nos^{RC}/nosRD* (Curtis et al., 1997). Larvae mutant for *brat* were generated using *brat^{11}*/Df(2L) *TE37C-7* (Frank et al., 2002; Sonoda and Wharton, 2001) or the strong hypomorphic combination *brat^{1}/brat^{11}* (Sonoda and Wharton, 2001). Larvae mutant for *pum* were generated using the strong hypomorphic combination *pum^{ET7}/pum^{ET9}* (Forbes and Lehmann, 1998). For RNAi and overexpression experiments, UAS transgenes were used in single copy. Animals were maintained at 25 °C except in experiments using *ppk-GAL4* and in *hid* epistasis experiments, which were performed at 29 °C to increase GAL4 efficiency.

For MARCM, *FRT40 brat^{11}* flies (Frank et al., 2002) were mated to *elav-GAL4*, *UAS-mCD8:GFP*, *hs-FLP*; *FRT40A tubP-GAL80* flies (Lee and Luo, 2001). Embryos were collected for a 2 hour period and aged for 3 h at 25 °C. Embryos were then heat-shocked at 39 °C for 50 min, allowed to recover for 30 min at 25 °C, then heat-shocked again at 39 °C for 45 min. Animals were reared at 18 °C until the late third (wandering) larval stage, when GFP-positive clones were imaged.

Imaging and quantification of dendrite and bouton morphology

Live imaging analysis was performed as previously described (Parrish et al., 2007a) except that larvae were mounted in halocarbon oil and imaged on a Leica SPE confocal microscope using a 40×/1.25 NA oil objective. The total number of terminal branches, mean branch length, terminal branch length, as well as the number of branches lost or gained between two time points was quantified in Z series projections of a single ddaC neuron by manual counting and by analyzing tracings of neurons created with NeuronJ (Meijering et al., 2004). All dendritic termini visible in the field of view were analyzed.

Unless otherwise noted, dendrite and bouton morphology were examined in wandering larval stages, corresponding to approximately 108–120 h after egg laying at 25 °C. Morphology was analyzed in larval filet preparations (Ye et al., 2004) immunostained with 1:350 Alexa Fluor 488 rabbit anti-GFP (Invitrogen), mounted in 70% glycerol, and imaged on a Leica SP5 confocal microscope using a 40×/1.25 NA oil objective (da neurons) or the 40× objective with 1.5× zoom (NMJ boutons). The total number of terminal branches was quantified in projections of individual ddaC neurons from the second through fifth abdominal segment as previously described (Lee et al., 2003). For wild-type ddaC neurons visualized using either *GAL4^{477}* or *ppk-GAL4* to express mCD8-GFP, approximately 350 terminal branches are routinely detected within the field of view. For bouton analysis, the NMJ lying at the interface of muscle 6/7 within the second and third abdominal segment was imaged. The total number of synaptic boutons per NMJ was determined separately for the second and third abdominal segments. Statistical significance was determined using the Student's *t*-test.

Immunofluorescence

Wandering larvae (approximately 108–120 h after egg laying at 25 °C) were filleted, fixed in 4% EM grade formaldehyde (Polysciences), and incubated overnight at 4 °C with the following primary antibodies in PBS/0.1% Triton X-100/5% normal goat serum (NGS): 1:20 mouse anti-cut (Developmental Studies Hybridoma Bank [DSHB]); 1:500 mouse anti-Futsch (DSHB); 1:10 mouse anti-Syt (DSHB); 1:100 mouse anti-Dlg (DSHB); 1:350 rat anti-Brat^{333} (Sonoda and Wharton, 2001); 1:200 rabbit anti-Brat (Cho et al., 2006); 1:100 mouse anti-Hid (gift from H. Steller); 1:100 rabbit anti-activated caspase (Trevigen). The following secondary antibodies (Invitrogen) were incubated overnight at 4 °C in PBS/0.1% Triton X-100/5% NGS: 1:700 Alexa Fluor 568 goat anti-mouse, 1:500 Alexa Fluor 488 goat anti-mouse; 1:1000 Alexa Fluor 546 goat anti-rat; 1:500 Alexa 568 goat anti-rabbit. For each experiment, all neurons were imaged at the same settings on a Leica SPE confocal microscope with a 63×/1.4 NA oil objective. For anti-Hid and anti-Cut immunostaining, fluorescence intensity was measured within a region of interest (ROI) corresponding to the cell nucleus and normalized to the volume of the cell nucleus using Velocity software. Values reported represent the average of 15–33 neurons from each genotype relative to a comparable number of neurons from the corresponding wild-type control. Statistical significance was measured by performing the Student's *t*-test.

Results

nos and pum are required for elaboration and stabilization of dendritic branches during late larval growth

The reduction in dendrite branching complexity in *nos* mutant class IV da neurons is first apparent during the third larval instar, indicating that *nos* is not required for the initial elaboration of the dendritic tree (Brechbiel and Gavis, 2008). To determine what role *nos* plays in dendrite morphogenesis, we first performed a time course analysis of dendrite morphology throughout the third larval instar in fixed larval preparations. The dorsal-most class IV da (ddaC) neurons from wild-

type and *nos* mutant larvae were visualized with the mCD8-GFP membrane marker expressed using the GAL4/UAS system with the class IV da neuron-specific *GAL4*^{477} driver. In addition, we analyzed ddaC neurons in which *nos* expression was knocked down by using *GAL4*^{477} to express a *UAS-nosRNAi* transgene. At 72 h after egg laying (AEL), corresponding to the early third larval instar, *nos* mutant neurons and *nos*^{RNAi} neurons are indistinguishable from control neurons. However, at 96 h AEL, or mid third larval instar, a few da neurons in each *nos* mutant or *nos*^{RNAi} larva show reduced higher order branching as monitored by the quantification of branch termini. This phenotype increases in severity and is exhibited by more neurons per larva as larval development progresses (data not shown; Brechbiel and Gavis, 2008). These results suggest that *nos* is required for the extension of new branches during larval growth, the maintenance of existing branches, or both.

To distinguish among these possibilities, we monitored dendrite dynamics of individual ddaC neurons by imaging live larvae first at 92 h AEL and then 17 h later, at 109 h AEL. This time window encompasses the onset of the *nos* mutant phenotype and provides sufficient opportunity to observe branch extension and retraction events. In preliminary experiments, we noticed that genetically *nos* mutant larvae pupate prior to 109 h AEL. This early pupariation defect in *nos* mutant larvae may reflect asynchronous development from wild-type larvae. To ensure that our live imaging analysis accurately compared developmental time points between *nos* deficient and control neurons, *nos* was depleted specifically in class IV da neurons by *GAL4*^{477}-mediated expression of *UAS-nosRNAi*. Consistent with the time course analysis in fixed tissue, live imaging at 92 h AEL shows no difference in the number of dendritic termini in *nos* deficient neurons compared to wild-type neurons. At 109 h AEL, however, *nos* RNAi results in fewer dendritic branches as compared to wild-type neurons.

To determine whether the apparent reduction in branching reflects loss of previously established branches, we monitored the net change in dendrite number in ddaC neurons between the two time points. Quantification shows that there is a net increase in the number of dendritic termini in wild-type neurons (Figs. 1A, B, G), while there is net decrease in *nos*^{RNAi} neurons (Figs. 1C, D, G). Since Nos functions with Pum to control dendrite development (Ye et al., 2004), we investigated whether *pum* mutant neurons exhibit similar dendrite dynamics to *nos* deficient neurons. Live imaging reveals that *pum* mutant neurons also exhibit a net loss of dendritic branches over 17 h (Figs. 1E, F, G). The extent of this loss exceeds that observed in *nos* deficient neurons, most likely due to the incomplete knockdown

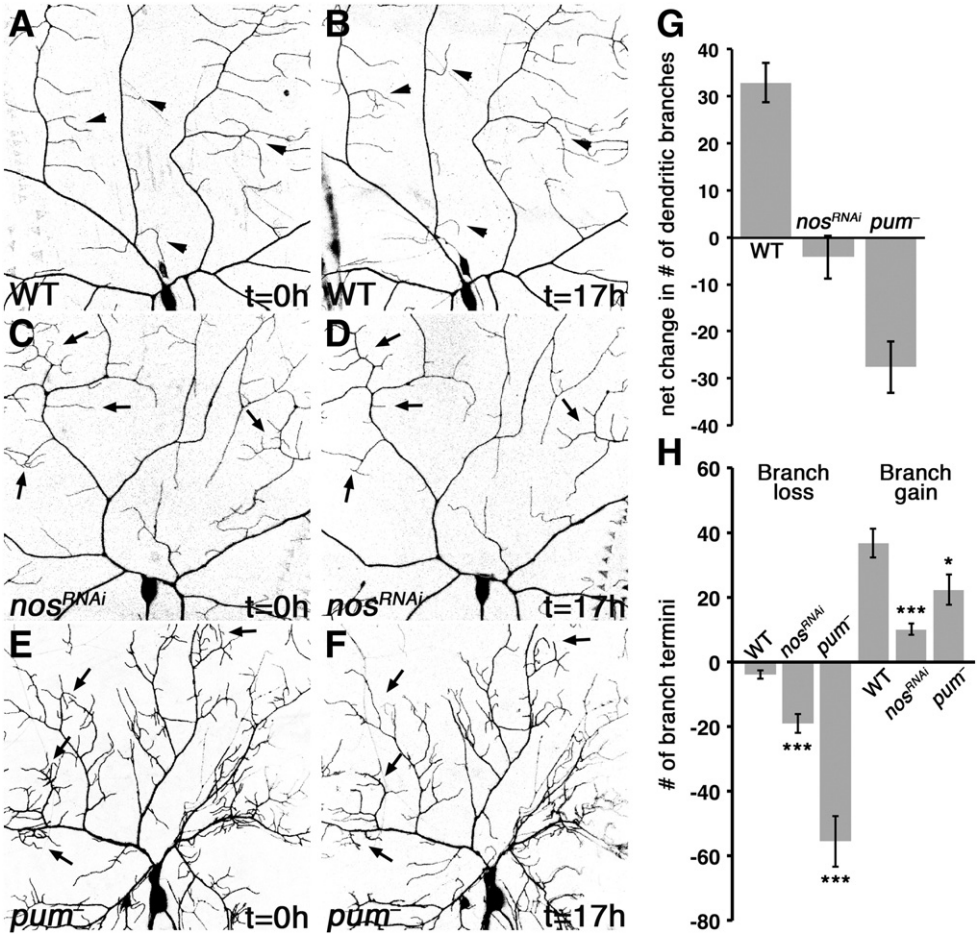

Fig. 1. *nos* and *pum* are required for dendritic branch stabilization. (A–F) Confocal z series projections of class IV da neurons marked using *GAL4*^{477} to drive expression of *UAS-mCD8:GFP*. (A, B) A ddaC neuron from a wild-type (WT) larva was imaged at 92 h AEL (t = 0 h; A) and again at 109 h AEL (t = 17 h; B). (C, D) A ddaC neuron from a larva expressing *UAS-nosRNAi* driven by *GAL4*^{477} (*nos*^{RNAi}) imaged at 92 h AEL (C) and again at 109 h AEL (D). (E, F) A ddaC neuron from a *pum* mutant (*pum*$^{-}$) larva imaged at 92 h AEL (E) and again at 109 h AEL (F). Arrowheads indicate examples of new branch growth and arrows indicate examples of branch loss during the 17 h time period. Both *pum* and *nos* mutant da neurons have a dendritic field coverage defect, such that dendrites are closer to the cell body than in wild-type neurons (Ye et al., 2004). *nos* RNAi produces a weaker phenotype than *nos* and *pum* mutations, resulting in less of a coverage defect. Thus, the *pum* mutant neurons are more compressed and the field of view shown therefore encompasses more of the distal branches for the *pum* mutant neuron than for the *nos*^{RNAi} neuron. (G) Quantification of the net change in total number of terminal branches over 17 h: WT (n = 10), *nos*^{RNAi} (n = 9), *pum*$^{-}$ (n = 10). (H) Quantification of the number of branches lost and number of new branches gained over 17 h: WT (n = 6), *nos*^{RNAi} (n = 6), *pum*$^{-}$ (n = 7). Here and in all subsequent figures, values are the mean ± SEM. $^{*}p \le 0.05$; $^{**}p \le 0.01$; $^{***}p \le 0.001$ as determined by the Student's *t*-test.

of *nos* by RNAi. The net decrease in dendritic branch termini indicates that both *nos* and *pum* play a role in maintaining existing branches during the late third larval instar.

To determine whether Nos and Pum are also required for the growth of new dendritic branches during the late third larval instar, we monitored the dynamics of individual dendrites within each neuron. We observed retraction of numerous branches in nos^{RNAi} and *pum* mutant neurons within the 17 hour time period, whereas little or no retraction was observed in wild-type neurons. Although wild-type control neurons add many new branches during this time, nos^{RNAi} neurons add significantly fewer branches. A strong trend toward less new growth was observed in *pum* mutants as well (Figs. 1H). Therefore Nos and Pum are required for stabilization of existing dendritic branches as well as for outgrowth of new branches during the mid to late third larval instar.

Hid is upregulated in nos and pum mutant neurons

Upon puparium formation, class IV da neurons are extensively pruned and remodeled. During this process, primary branches undergo severing and local degeneration, and are then replaced with new dendritic branches necessary for establishing connections in the adult animal. Components of the apoptotic pathway have been shown to play a role in da neuron remodeling during metamorphosis (Kuo et al., 2006; Rumpf et al., 2011; Williams and Truman, 2005b; Williams et al., 2006). Moreover, Nos has previously been implicated in translational repression of the proapoptotic factor Hid in developing germ cells (Sato et al., 2007). Although Hid has not been implicated in pruning during metamorphosis, we hypothesized that the excessive retraction phenotype of *nos* and *pum* deficient neurons could be due to an inappropriate production of Hid and other apoptotic machinery in da neurons. Anti-Hid immunofluorescence detects little or no Hid protein in ddaC neurons in wild-type wandering larvae (Figs. 2A–C). In contrast, Hid levels are elevated in *nos* mutant, nos^{RNAi}, and *pum* mutant neurons, with Hid often concentrated in one or two foci within the nucleus (Figs. 2D–I; Fig. S1). To determine whether this increase in Hid contributes to the loss of dendrites in *nos* deficient neurons, we tested the effect of lowering *hid* gene dosage on dendrite morphology in nos^{RNAi} neurons. The loss of dendritic termini in nos^{RNAi} da neurons is fully rescued when larvae are heterozygous for the H99 chromosomal deficiency that removes the *hid* locus (nos^{RNAi}; *H99*/+; Figs. 2J–M). This effect is specific to *nos* deficient neurons, as dendrite number in ddAC neurons from H99/+ larvae is indistinguishable from wild-type (data not shown). Moreover, Hid levels are restored to wild-type levels in nos^{RNAi}; *H99*/+ neurons, consistent with the restoration of branch termini (Fig. S1).

Upon dendrite severing, caspases are activated locally within the severed dendrites to promote their removal (Williams et al., 2006). We do not, however, detect activated caspase within *nos* or *pum* deficient ddaC neuron dendrites using immunofluorescence (data not shown). Consistent with this result, *nos* and *pum* mutant neurons do not exhibit the dendrite severing that is characteristic of pruning during metamorphosis. While we cannot definitively rule out a role for caspases in contributing to the *nos* mutant phenotype, our results

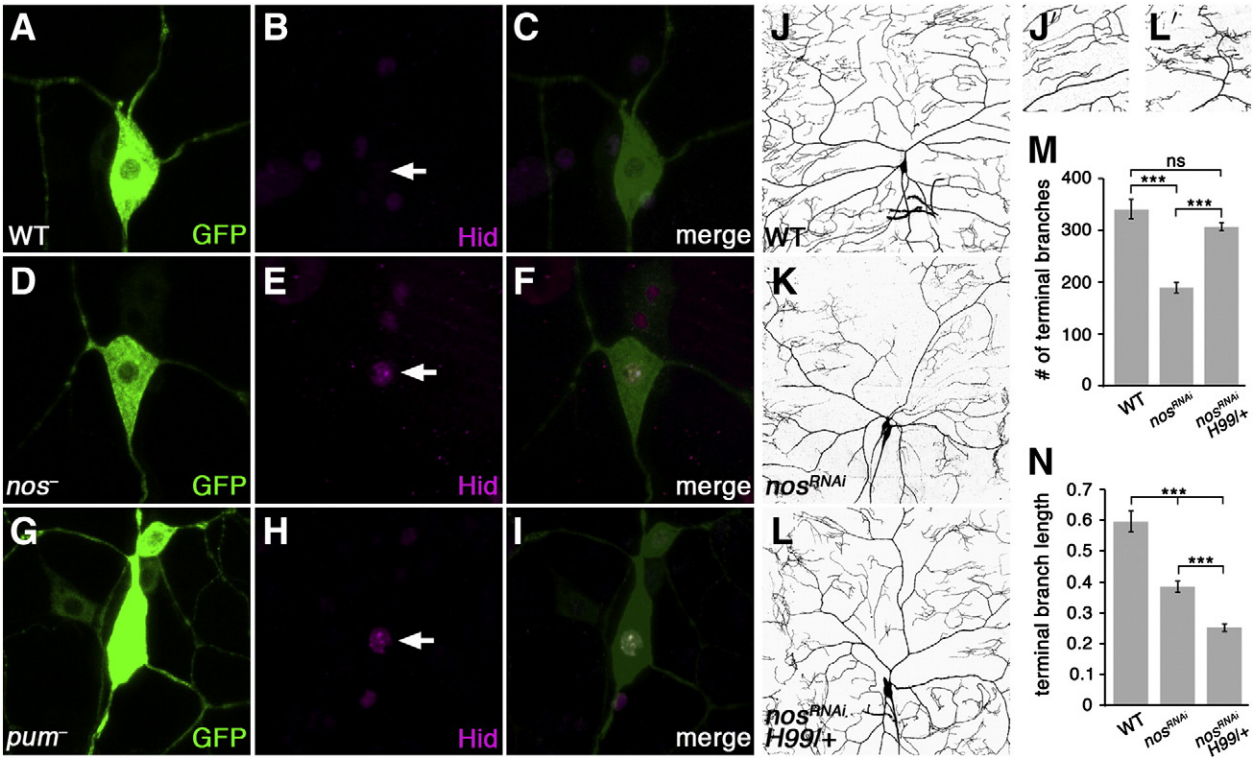

Fig. 2. Nos and Pum repress Hid expression. (A–I) Confocal z series projections of ddaC neurons from wild-type (WT; A–C), *nos* mutant (nos^{-}; D–F) and *pum* mutant (pum^{-}; G–I) larvae stained with anti-GFP antibody to detect the mCD8-GFP marker (green) and anti-Hid antibody (magenta). Enlargements of the region of the cell body are shown. The intensity of the green channel is lower in the merged images (C, F, I) to show Hid expression. Quantification of fluorescence intensity (see Materials and methods) shows that relative to wild-type neurons (n = 29), Hid is upregulated 8 fold in *nos* mutant neurons ($p = 1 \times 10^{-7}$) and 6 fold in *pum* mutant neurons ($p = 2 \times 10^{-8}$). (J–L) ddaC neurons with $GAL4^{477}$ driving expression of mCD8-GFP alone (WT; J), with nos^{RNAi} (K), and with nos^{RNAi} in larvae heterozygous for the *H99* deficiency (L). (J′, L′) Enlargements of terminal branches in WT (J′) and nos^{RNAi}/*H99* (L′) ddaC neurons show shorter and clustered terminal branches in *H99*/nos^{RNAi} neurons. (M) Quantification of the total number of terminal branches: WT (n = 10); nos^{RNAi} (n = 23); nos^{RNAi}/*H99*(n = 30). (N) Quantification of the average terminal branch length: WT (n = 102); nos^{RNAi} (n = 101); nos^{RNAi}/*H99* (n = 102). Note that although the cell body of a class I da neuron is often weakly labeled when $GAL4^{477}$ is used to express nos^{RNAi} (K), class IV da neuron dendrites are easily distinguished from class I dendrites for quantification.

suggest that *hid* is a target of repression by Nos and Pum in da neurons and that accumulation of Hid in *nos* and *pum* mutant neurons results in branch retraction by a caspase-independent mechanism.

In contrast to the long and evenly spaced dendritic branches of control ddaC neurons, *nos* deficient neurons have shorter terminal dendritic branches that tend to cluster together (Fig. 2N), suggesting that *nos* promotes branch length and regulates dendritic spacing. Lowering *hid* gene dosage does not rescue the defect in terminal branch length or branch spacing, however, and terminal branches are significantly shorter in *nosRNAi/H99* neurons as compared to both control and nos^{RNAi} neurons (Figs. 2J', L', N). Thus, while *hid* appears to act downstream of Nos to regulate dendrite maintenance and retraction, regulation of branch length and spacing is likely mediated by other Nos targets or cofactors.

Nos and Pum regulate Cut expression in Class IV da neurons

The defects associated with terminal dendrite length in *nos* deficient neurons occur independently of apoptotic machinery suggesting that additional Nos targets promote branch length. The distinct dendritic patterns and morphologies exhibited by different classes of da neurons are controlled in part by the level of the transcription factor Cut (Grueber et al., 2003; Jinushi-Nakao et al., 2007; Li et al., 2004). Class IV da neurons express intermediate levels of Cut protein during both embryonic and larval development (Grueber et al., 2003) suggesting that Cut functions not only during the initial differentiation of these neurons, but also during their subsequent development to specify their characteristic dendritic patterns. Similarly to *nos* and *pum* mutants, *cut* mutant class IV da neurons show reduced higher order dendritic branching and reduced branch length. Moreover, overexpression of *nos* and *pum* in class IV da neurons results in a severe loss of dendritic branching and a dramatic reduction in the length of individual branches (Ye et al., 2004); a similar defect is produced by *cut* overexpression (Grueber et al., 2003; Jinushi-Nakao et al., 2007). The similarity in these overexpression phenotypes suggests that Nos and Pum might regulate dendritic branching and promote branch length through an effect on *cut* expression. Anti-Cut immunofluorescence shows that overexpressing *nos* or *pum* using *UAS-nos-tub3′ UTR* and *UAS-pum* transgenes, respectively, driven by $GAL4^{477}$ results in an increase in Cut protein levels within ddaC neurons (Figs. 3A–C). We investigated whether the elevated Cut levels contribute to the loss of dendrites in neurons overexpressing *nos* or *pum* by genetically removing one copy of *cut* with the strong hypomorphic cut^{145} allele (Grueber et al., 2003). Lowering Cut levels in this way has no effect on its own but partially suppresses the loss of dendritic branches and branch length defects associated with *nos* and *pum* overexpression (Figs. 4A–E and data not shown), suggesting that *cut* functions downstream of *nos* and *pum* in dendrite development.

We next investigated whether Cut levels are affected in neurons deficient for *nos* or *pum*. Conversely to *nos* overexpression, *nos* mutant and nos^{RNAi} neurons have decreased levels of Cut protein compared to wild-type neurons (Figs. 3D, E). In contrast, *pum* mutant neurons express Cut protein at higher levels than wild-type neurons (Figs. 3F). Thus, while the phenotypes due to overexpression of *nos* and *pum* may result in part from inappropriate upregulation of Cut expression, the different effects on Cut protein levels in *nos* versus *pum* mutant neurons suggest that Nos and Pum regulate distinct targets that affect Cut level differentially within ddaC neurons. GAL4/UAS-mediated overexpression of Cut produces a more severe phenotype than is observed in *pum* mutant neurons (Grueber et al., 2003; Jinushi-Nakao et al., 2007). However, modulation of Cut activity by

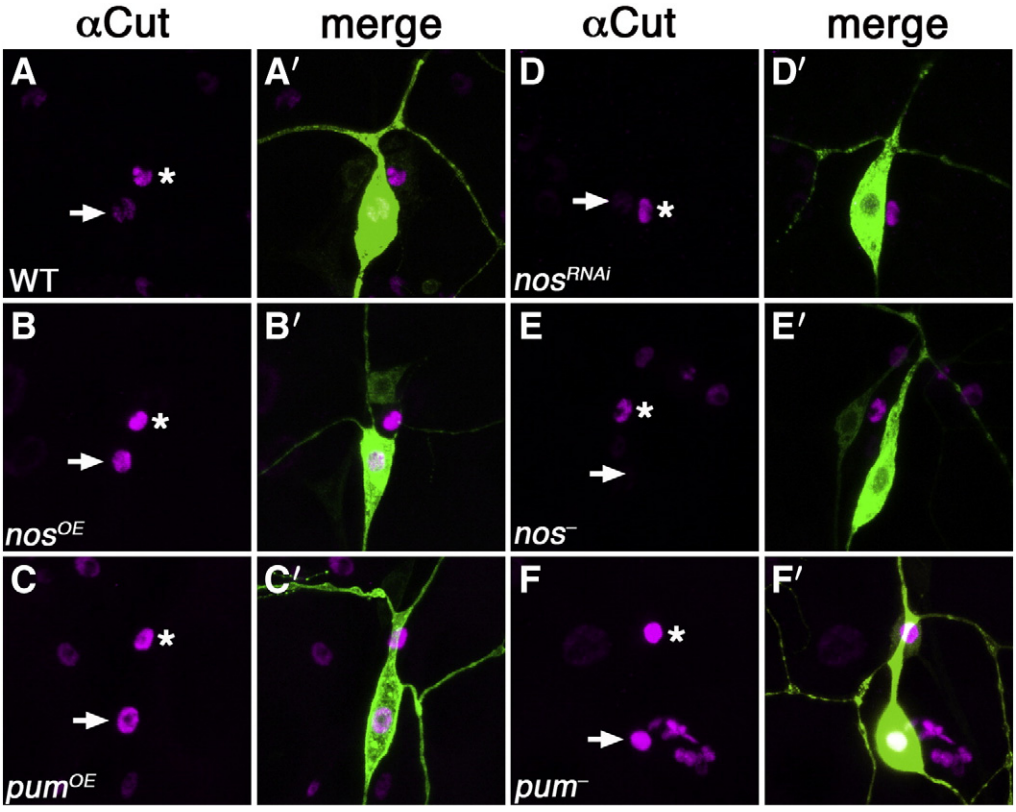

Fig. 3. Nos and Pum differentially influence Cut expression. Anti-Cut (magenta) and anti-GFP (green) immunostaining of ddaC neurons marked with mCD8-GFP. (A, A') Wild-type (WT) ddaC neurons express intermediate levels of Cut. Cut levels are increased relative to wild-type in *nos* overexpressing (nos^{OE}; B, B'), *pum* overexpressing (pum^{OE}; C, C'), and pum^{-} ddaC neurons (F, F'). Cut levels are reduced relative to wild-type in ddaC neurons expressing *nosRNAi* (D, D') and in nos^{-} ddaC neurons (E, E'). Nuclei from representative ddaC neurons for each genotype are indicated with arrows. For comparison, class III neurons, which express high levels of Cut, are indicated with an asterisk. Quantification of fluorescence intensity (see Materials and methods) shows that relative to wild-type neurons, Cut is upregulated 5 fold in nos^{OE} neurons ($p=0.001$) and 6 fold in pum^{OE} ($p=5\times10^{-5}$) and *pum* mutant ($p=9\times10^{-6}$) neurons. Cut levels are decreased 2 fold in nos^{-} neurons ($p=0.007$) and nos^{RNAi} ($p=0.03$) neurons.

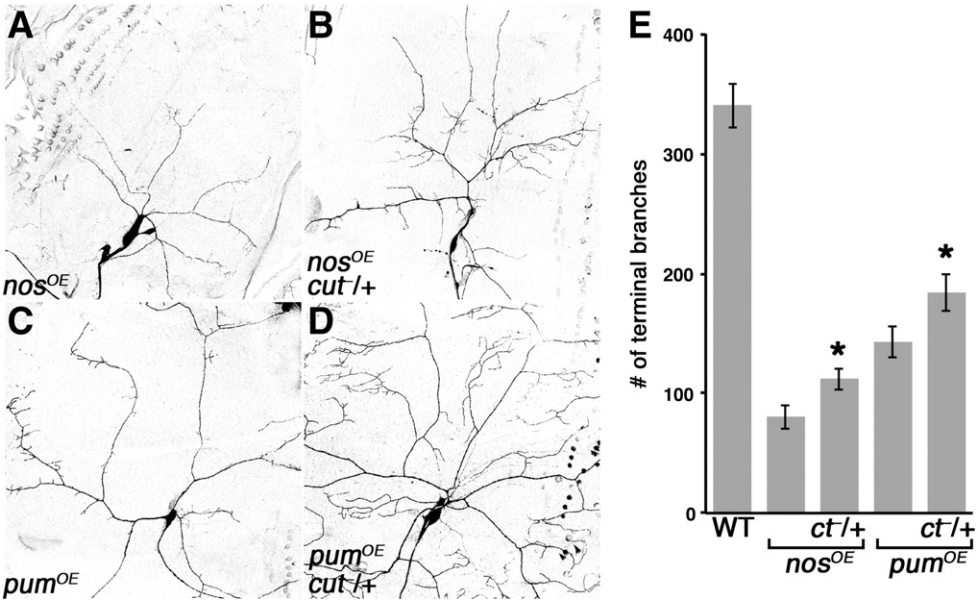

Fig. 4. *cut* interacts genetically with *nos* and *pum*. (A–D) Larval ddaC neurons visualized using $GAL4^{477}$ to express mCD8-GFP. $GAL4^{477}$-mediated overexpression of *nos* (nos^{OE}; A) or *pum* (pum^{OE}; C) results in loss of higher order branches. Reduction of *cut* levels by heterozygosity for the ct^{c145} allele (B,D) partially restores branching morphogenesis. (E) Quantification of the total number of terminal branches: nos^{OE} (n = 13), $ct^{-}/+$; nos^{OE} (n = 22), pum^{OE} (n = 20), $ct^{-}/+$; pum^{OE} (n = 25).

other factors is required for generating the distinct dendritic patterns of the different classes of da neurons (Jinushi-Nakao et al., 2007) and these factors may be missing from *pum* mutant neurons.

Brat is required for dendritic development of ddaC neurons

To survey the role of RNA-binding proteins in neuronal development, we performed an RNAi screen in which we systematically knocked down the expression of the majority of the annotated *Drosophila* RNA binding proteins specifically in class IV da neurons (E.C.O. and E.R.G. unpublished). The screen, in which *UAS-RNAi* transgenes were expressed in class IV da neurons using $GAL4^{477}$, will be described elsewhere. Among the positive candidates from this screen, we identified *brat*. Knockdown of *brat* using either of two different *UAS-bratRNAi* transgenes results in a loss of higher order dendritic branches and a reduction in the overall field of coverage in ddaC neurons as compared to wild-type neurons (Figs. 5A, B and data not shown). Loss of higher order branching was also observed using another class IV da neuron-specific driver, *ppk-GAL4* (data not shown).

A requirement for *brat* in dendrite morphogenesis was confirmed using two *brat* mutant alleles. Viable larvae were obtained for transheterozygous combinations of the $brat^{1}$ and $brat^{11}$ alleles and for the $brat^{1}$ allele in trans to a deficiency spanning the *brat* locus. Similarly to *brat* RNAi, these mutant combinations result in a loss of higher order dendritic branching in ddaC neurons (Figs. 5F–H). Moreover, $brat^{11}$ mutant clones generated by the Mosaic Analysis with a Repressible Cell Marker (MARCM) method (Lee and Luo, 2001) show reduced dendritic complexity and field coverage as compared to control ddaC mitotic clones (Figs. 5C, D, E), confirming that *brat* is required cell autonomously in class IV da neurons for dendrite development. Consistent with these results, anti-Brat immunofluorescence detects cytoplasmic Brat protein in the ddaC neuron cell body (Figs. 5I–K).

In addition to class IV da neurons, class III da neurons require *nos* and *pum* for dendrite development. In contrast, *nos* and *pum* are dispensable in class I and class II da neurons (Ye et al., 2004). Analysis of $brat^{11}$ MARCM clones shows no effect on the development of class I, II and III da neurons (Fig. S2). Thus, the requirement for *brat* appears to be limited to class IV da neurons, although we cannot rule out the possibility that residual function of the hypomorphic $brat^{11}$ allele suffices in the other classes.

Brat functions with nos and pum to regulate dendrite development

The requirement for *brat* in class IV da neurons suggests that Brat may function in concert with Nos and Pum to mediate translational repression during dendrite morphogenesis. We therefore tested whether *brat* interacts genetically with *nos* and *pum* in da neurons. Overexpression of *brat* using a *UAS-brat* transgene driven by $GAL4^{477}$ results in reduced dendritic complexity and field coverage (Fig. 6A) and similar results were obtained with *ppk-GAL4* (Figs. S4E, F, H). Reducing *nos* function using RNAi or by mutation of one copy of *nos* suppresses the dendritic defects caused by *brat* overexpression (Figs. 6B, C, K). Similarly, reducing *pum* function suppresses dendritic defects associated with *brat* overexpression (Figs. 6D, E, K).

The suppression of the *brat* overexpression phenotype by reducing *nos* and *pum* function suggests that *brat* functions either upstream of or together with *nos* and *pum* to regulate dendrite morphogenesis. In order to distinguish between these two possibilities, we took advantage of *nos* and *pum* overexpression phenotypes to perform epistasis experiments. *nos* and *pum* overexpression driven by *ppk-GAL4* results in a dramatic loss of dendritic branching (Figs. 6F, I respectively). Removing one copy of *brat* has no effect on its own, but partially suppresses the *nos* overexpression phenotype and more substantially suppresses the *pum* overexpression phenotype (Figs. 6G, J, K and data not shown). Such partial suppression of *nos* overexpression is also observed when *pum* function is reduced (Fig. 6H). We suspect that *nos* overexpression can cause some degree of toxicity, as is observed in other tissues (Clark et al., 2002). Together, these results provide evidence that *brat*, *pum* and *nos* function together to regulate dendritic development.

Hid but not Cut expression is affected in brat deficient neurons

Results presented above suggest that Nos and Pum repress translation of *hid* in da neurons. To determine whether Brat also contributes to regulation of *hid*, we assayed Hid protein levels in *brat* mutant neurons. Anti-Hid immunofluorescence shows elevated Hid protein levels

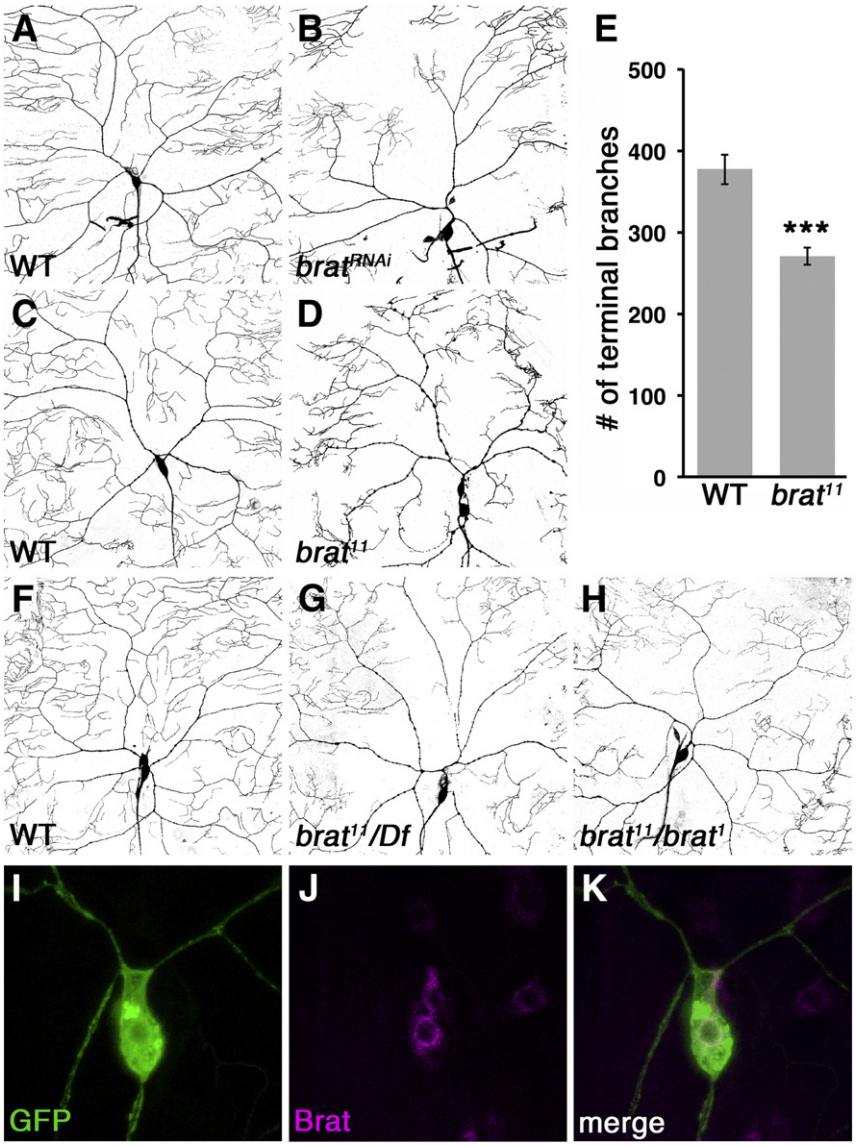

Fig. 5. *brat* plays a cell autonomous role in da neuron dendrite morphogenesis. (A, B) Larval ddaC neurons expressing *UAS-mCD8:GFP* alone (A) or together with *UAS-brat RNAi* (B) using $GAL4^{477}$. (C, D) Wild-type control (WT; C) and $brat^{11}$ (D) ddaC MARCM clones with *UAS-mCD8:GFP* expressed by *elav-GAL4*. (E) Quantification of terminal branch number in MARCM clones: WT (n = 9); $brat^{11}$ (n = 14). (F–H) ddaC neurons from wild-type (F) $brat^{11}$/Df(2L)*TE37C-7* (G), and $brat^{11}/brat^{1}$ (H) larvae. *UAS-mCD8:GFP* is expressed by the *ppk-GAL4* driver. (I–K) Larval ddaC neuron stained with anti-GFP antibody to detect the mCD8-GFP marker (green) and anti-Brat antibody (magenta). Enlargement of the region of the cell body is shown, with Brat detected in the cytoplasm. The intensity of the green channel was lowered in the merged image (K). Brat is also detected at lower levels in other cells in the field of view.

in neurons from $brat^{11}$/*Df* and $brat^{11}/brat^{1}$ larvae as compared to wild-type neurons (Fig. S3), consistent with repression of *hid* by a complex involving Nos, Pum, and Brat.

We investigated whether Brat, like Nos and Pum, might also regulate *cut* expression in da neurons. Anti-Cut immunofluorescence shows that *brat* overexpression results in elevated levels of Cut protein in ddaC neurons, similar to neurons overexpressing either *nos* or *pum*. However, Cut expression is unaffected in *brat* mutant neurons (Fig. S3). Additionally, reducing *cut* function does not suppress the loss of higher order branches in neurons overexpressing *brat* (Figs. S4A, B, D). Taken together, our data suggest that *brat* is not involved in regulating Cut expression.

d4EHP interacts with brat during dendrite morphogenesis

In the early *Drosophila* embryo, the Nos/Pum/Brat complex represses translation of *hb* mRNA by a cap-dependent mechanism. d4EHP, an eIF4E-like cap binding protein, facilitates this repression by simultaneously interacting with Brat and the 7-methyl guanosine cap structure at the 5′ end of *hb* mRNA (Cho et al., 2006). In our RNAi screen, *d4EHP* RNAi produced a reproducible but weak defect in the dendrite arborization pattern, where termini are shortened and unevenly distributed creating dendrite free regions within the dendritic tree (data not shown). In larvae mutant for the viable $d4EHP^{CP53}$ mutant allele, the number of dendritic termini is not affected in ddaC neurons, but they display defects in dendrite patterning whereby branches are shortened and unevenly distributed, similar to $d4EHP^{RNAi}$ neurons (Fig. S5). Due to the hypomorphic nature of the $d4EHP^{CP53}$ allele and the potentially incomplete knockdown of *d4EHP* via RNAi, it remains possible that a null mutant allele would produce more severe dendritic defects.

We next investigated whether *d4EHP* interacts genetically with *brat* to regulate dendrite morphogenesis in ddaC neurons. Reducing *d4EHP* function partially rescues the dendritic branching defect caused by *brat* overexpression (Figs. S4A, C, D). Moreover, overexpression of a mutant form of *brat* that is unable to bind d4EHP (Harris et al., 2011) results in a weaker dendrite morphogenesis defect than overexpression of wild-type *brat* (Figs. S4F, G, H). Taken together, the overexpression

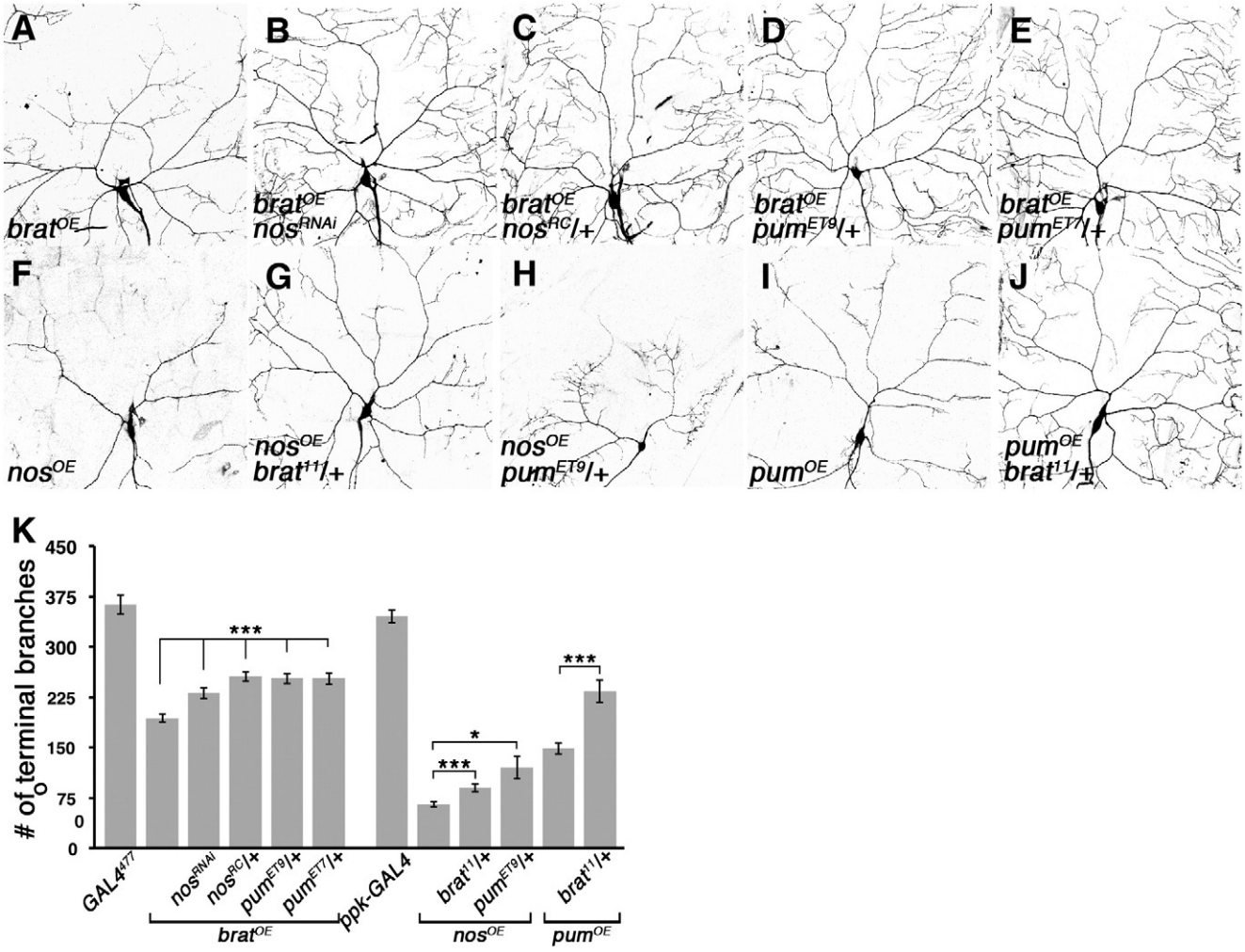

Fig. 6. *nos*, *pum* and *brat* genetically interact to promote dendrite morphogenesis. (A–J) Larval ddaC neurons overexpressing *brat* ($brat^{OE}$), *nos* (nos^{OE}) or *pum* (pum^{OE}). (A–E) $GAL4^{477}$ was used to express both *UAS-mCD8:GFP* and *UAS-brat*. Neurons overexpressing *brat* (A) have reduced higher order branching and reduced dendritic field coverage. When *nos* function is reduced by RNAi (B) and in larva heterozygous for nos^{RC} (C), pum^{ET9} (D), or pum^{ET7} (E), dendritic field coverage is restored and the dendritic branching defect is partially rescued. (F–J) *ppk-GAL4* was used to express *UAS-mCD8:GFP* and either *UAS-nos-tub3′UTR* (F–H) or *UAS-pum* (I, J). Neurons overexpressing *nos* (F) or pum (I) elaborate few dendrites. In larvae heterozygous for $brat^{11}$ (G, J) or pum^{ET9} (H), the defects caused by *nos* or *pum* overexpression are partially rescued. (K) Quantification of the total number of terminal branches: $brat^{OE}$ (n=31); $brat^{OE}$ with *nosRNAi* (n=13); $brat^{OE}$ in nos^{RC} heterozygotes (n=24); $brat^{OE}$ in pum^{ET7} heterozygotes (n=20); $brat^{OE}$ in pum^{ET9} heterozygotes (n=21); nos^{OE} (n=24), nos^{OE} in $brat^{11}$ heterozygotes (n=28); nos^{OE} in pum^{ET9} heterozygotes (n=7); pum^{OE} (n=20); pum^{OE} in $brat^{11}$ heterozygotes (n=22).

and epistasis analyses show that *brat* genetically interacts with *d4EHP* in da neurons to regulate dendrite development.

Brat functions presynaptically at the NMJ to regulate bouton morphogenesis

In contrast to their collaborative role in da neurons, Nos and Pum function in opposition to one another to regulate both bouton morphogenesis and the electrophysiological properties of the NMJ (Menon et al., 2009). Anti-Brat immunofluorescence detects Brat in the larval NMJ, suggesting a role for Brat in NMJ development. To begin to distinguish how Brat might function at the NMJ, we examined Brat localization relative to the presynaptic marker, Synaptotagmin-GFP (Syt-GFP) and the postsynaptic marker Discs large-YFP (Dlg-YFP). Immunofluorescence detection of Brat together with each marker shows that Brat colocalizes presynaptically with Syt-GFP, but not postsynaptically with Dlg-YFP (Figs. 7A–F).

To determine whether the presence of Brat in the NMJ reflects its function there, we examined $brat^{11}/brat^{1}$ and $brat^{11}/Df$ third instar larvae immunostained for either endogenous Syt or Dlg to visualize boutons. Boutons in *brat* mutant NMJs are often misshapen, fused or enlarged as compared to wild-type NMJs (Figs. 7J–L). Quantification of bouton number, most easily performed using anti-Syt immunofluorescence, shows a statistically significant reduction in bouton number in *brat* mutant relative to wild-type NMJs (Fig. 7N). This defect is similar to the defect observed in *pum* mutant NMJs (Menon et al., 2004).

We targeted *brat* RNAi to the pre- or post-synaptic compartments to ascertain where *brat* function is required. Presynaptic expression of *brat* RNAi using *OK6-GAL4* produces a *pum*-like phenotype, with a reduction in bouton number, as well as misshapen, enlarged or fused boutons as compared to wild-type NMJs. Similar results were obtained with two different *UAS-brat* RNAi lines (Figs. 7G–I, M). In contrast, *brat* RNAi expressed postsynaptically, using either the *Mef2-GAL4* or *Mhc82-GAL4* muscle drivers, does not produce overt bouton defects (data not shown). Both *Mef2-GAL4* and *Mhc82-GAL4* effectively drive the expression of a *UAS-mCherry* reporter indicating that they are indeed functional (data not shown). These results indicate that *brat* functions presynaptically to regulate bouton morphogenesis in the NMJ, consistent with the presynaptic localization of Brat protein. We conclude that *brat* plays a fundamental role in the development of synaptic boutons in the larval neuromuscular system.

The *brat* mutant NMJ phenotype resembles the phenotype of *pum* rather than *nos* mutant NMJs. We were unable, however, to test genetically whether *brat* functions with *pum* in bouton morphogenesis. Overexpression of *brat* either pre- or postsynaptically does not cause bouton morphogenesis defects (data not shown). While presynaptic *pum*

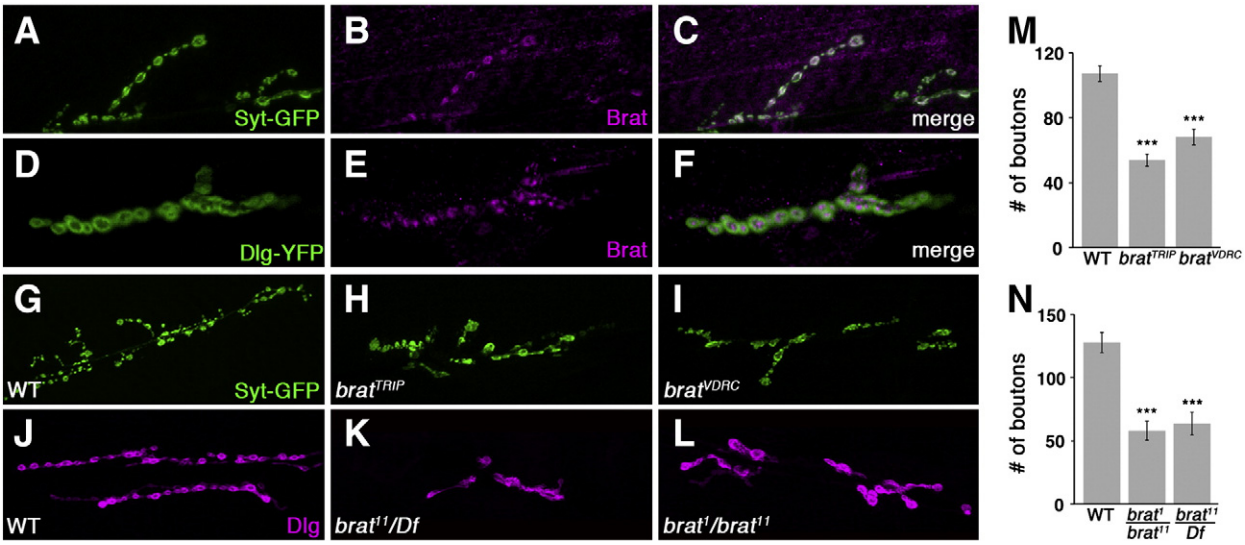

Fig. 7. *brat* function is required for bouton morphogenesis at the larval NMJ. Confocal z series projections of larval NMJs from muscle 6/7. (A–F) Immunofluorescence detection of Brat (magenta) together with (A) the presynaptic marker Syt-GFP (green) or (D) the postsynaptic marker Dlg-YFP (green). *UAS-Syt:GFP* was expressed using *OK6-GAL4*. Merged images (C, F) show that Brat expression is presynaptic. (G–I) Presynaptic expression of two different *UAS-brat* RNAi transgenes in larval NMJs from muscle 6/7 labeled with anti-GFP to detect Syt-GFP. Knockdown of *brat* results in fewer boutons than in the wild-type (WT) control. (J–L) Muscle 6/7 NMJs in WT (J) $brat^{11}$/Df(2 L)*TE37C-7* (K) and $brat^{1}/brat^{11}$ (L) larvae labeled by anti-Dlg immunofluorescence. (M) Quantification of the total number of boutons in WT (n = 16), $brat^{TRIP}$ (n = 23), and $brat^{VDRC}$ (n = 23) larvae from experiment shown in (G–I). (N) Quantification of boutons in WT (n = 12), $brat^{1}/brat^{11}$ (n = 14), and $brat^{11}/Df$ (n = 16) larvae visualized by immunostaining for endogenous Syt (not shown).

overexpression does produce a bouton defect (Menon et al., 2004), we were unable to generate animals with presynaptic *pum* overexpression that were also heterozygous for *brat* mutations. Nonetheless, our results suggest that *brat* functions presynaptically to regulate bouton morphogenesis and the similarity of the *brat* and *pum* mutant bouton phenotypes suggests that Brat and Pum function together, in opposition to Nos, to regulate bouton development in the larval NMJ.

Discussion

Post-transcriptional mechanisms of gene regulation such as translational control play a fundamental role in the development and function of the nervous system (Eberwine et al., 2001; Job and Eberwine, 2001; Martin, 2004; Mikl et al., 2010; Schuman et al., 2006). Genetic studies have identified roles for the translational repressors Nos and Pum in sensory neuron and NMJ morphogenesis, NMJ function, and motor neuron excitability, and Pum has been implicated in long-term memory (Baines, 2005). Understanding the selectivity of these regulators for different mRNA targets is essential to identify the cellular processes they regulate for neuronal morphogenesis and neural function. Here, we show that different combinations of Nos, Pum, and the co-factor Brat confer cell type-specific regulation during morphogenesis of *Drosophila* da sensory neurons and the NMJ.

In *Drosophila* class IV da neurons, dendritic arbors grow rapidly during the first larval instar to establish nonredundant territories that cover the larval body wall. During the second and third larval instars, da neuron dendrites add and lengthen higher order branches to maintain body wall coverage as the larva undergoes dramatic growth. Results from our live imaging analysis place the requirement for Nos and Pum during the third larval instar, indicating that Nos and Pum are not involved in the establishment of dendritic territories but rather in maintaining the density of terminal branches during late larval growth by promoting branch extension and preventing branch retraction. We cannot, however, rule out the possibility that branch stabilization depends on Nos and Pum activity earlier during larval development. We also provide evidence that this maintenance function of Nos and Pum depends on their regulation of the proapoptotic protein Hid. Nos has previously been proposed to repress *hid* mRNA translation in developing germ cells to suppress apoptosis, although requirements for Pum and Brat were not tested (Sato et al., 2007). Together, our data showing that Hid is elevated in *nos* and *pum* mutant da neurons and that both the upregulation of Hid and the loss of terminal branches in *nos* mutants are suppressed by reduction of *hid* gene dosage suggest that repression of *hid* mRNA translation by Nos and Pum is also crucial for dendrite morphogenesis. Biochemical analysis will be required to test this model directly.

In cultured *Drosophila* cells, Hid localizes to mitochondria and this localization is required for full caspase activation (Abdelwahid et al., 2007; Haining et al., 1999). By contrast, Hid protein is detected in the nucleus in *nos* and *pum* mutants. A similar nuclear accumulation has been proposed to sequester Hid in larval malphigian tubules and prevent apoptosis of this tissue during metamorphosis (Shukla and Tapadia, 2011). The nuclear accumulation of Hid may indeed explain why upregulation of Hid in *nos* and *pum* da mutants does not cause cell death. Nuclear Hid sequestration in *nos* and *pum* mutant neurons is also consistent with the apparent absence of activated caspase. How Hid causes dendrite loss in *nos* and *pum* mutant neurons remains to be determined but could involve activation of a pathway similar to injury induced dendrite degeneration, which resembles pruning but is caspase-independent (Tao and Rolls, 2011).

Nos and Pum were initially identified because of their role in translational repression of *hb* mRNA in the posterior region of the early embryo. There, the two proteins form an obligate repression complex, with Pum conferring the RNA-binding specificity and Nos, which is synthesized only at the posterior pole of the embryo, providing the spatial specificity (Thompson et al., 2007). More recent studies have shown that Nos and Pum are not obligate partners, however. In the ovary, Pum functions together with Nos in germline stem cells to promote their self-renewal, while Pum acts independently of Nos in progeny cystoblasts to promote their differentiation (Harris et al., 2011). In the NMJ, Pum and Nos work in opposition to one another to regulate both morphological and electrophysiological characteristics of synaptic boutons (Menon et al., 2009). While Hid levels are similarly elevated in *nos* and *pum* mutant da neurons, the differential effects on *cut* expression observed in the two mutants suggest that in addition to working together, Nos and Pum participate in separate complexes that target different mRNAs even within the same cell type. Presumably, additional factors that associate selectively with

Nos or Pum drive the formation of distinct complexes with different binding specificities. Pum represses *eIF4E* translation in the post-synaptic NMJ independently of Nos (Menon et al., 2004), suggesting that some of Pum's effects in da neurons could be through more global effects on translation.

A third cofactor, Brat, is required for Nos/Pum-dependent repression of *hb* mRNA in the early embryo and *paralytic* mRNA in motorneurons (Muraro et al., 2008; Sonoda and Wharton, 2001). However, Brat is not required for Nos/Pum-mediated repression of *cyclin B* mRNA in primordial germ cells or for Nos/Pum function in germline stem-cell maintenance (Harris et al., 2011; Sonoda and Wharton, 2001). Structural and molecular analyses have shown that Brat is recruited to the Nos/Pum/NRE ternary complexes through an interaction between its conserved NHL (NCL-1, HT2A, and LIN-41) domain and Pum (Edwards et al., 2003). The Brat NHL domain also mediates interaction of Brat with the eIF4E-binding protein d4EHP and mutations in Brat that abrogate this interaction partially disrupt translational repression of *hb*, suggesting a mechanism by which the Pum/Nos/Brat/NRE complex could repress cap-dependent initiation (Cho et al., 2006). Our results indicate that Brat also collaborates with Nos and Pum to regulate dendrite morphogenesis by a mechanism involving d4EHP interaction and that this requirement is cell type-specific. While genetic analysis suggests that Brat is required for Nos/Pum-mediated regulation of dendrite complexity and Hid expression in class IV da neurons, it is dispensible for Nos and Pum functions in class III da neurons. A similar cell type-specific requirement for Brat function in Nos/Pum-mediated repression within the CNS has been proposed based on the ability of *brat* mutants to counteract repression of *paralytic* mRNA due to Pum overexpression (Muraro et al., 2008). Since Brat is expressed throughout the dorsal cluster of larval sensory neurons (data not shown) and CNS, it is unclear whether the recruitment of Brat to the complex occurs only in certain cell types or whether its function in the complex is target dependent. In contrast to *nos* and *pum* mutants, however, *brat* mutants have no effect on *cut* expression, suggesting that Brat's role in translational regulation is in fact limited to a subset of Nos/Pum-dependent processes.

Our findings that Brat functions presynaptically in bouton formation and that *brat* and *pum* mutant NMJs exhibit similar defects in bouton formation suggest that Brat is selectively recruited by Pum, but not by Nos, to regulate distinct target mRNAs in bouton development. Similarly, Brat functions selectively with Pum in ovarian cystoblasts to promote differentiation (Harris et al., 2011), suggesting that a Pum/Nos/NRE ternary complex is not essential for recruitment of Brat. Pum and many of its homologs in other organisms, members of the large Puf (Pum/FBF) protein family, typically recognize sequences that contain a core UGUA motif, although features beyond the core element also influence target mRNA recognition (Bernstein et al., 2005). We have shown that Pum can also recognize a UGUG motif that is found in binding sites for the *C. elegans* Puf protein FBF (Menon et al., 2009). Thus, it is possible that the interaction of Pum with different binding sites dictates the assembly of the particular repression complex. Interactors like Brat might add an additional layer of regulation by altering the specificity or affinity of Pum for particular targets, thereby generating diverse cellular and morphological outputs within a particular cell type.

Supplementary materials related to this article can be found online at doi:10.1016/j.ydbio.2012.02.028.

Acknowledgments

We thank H. Ashe, A. Brand, N. Brown, I. Davis, W. Grueber, Y.N. Jan, K. Menon, D. St Johnston, R. Wharton, K. Zinn, the Bloomington *Drosophila* stock center, the Vienna *Drosophila* RNAi Center, and TRiP at Harvard Medical School (NIH/NIGMS R01-GM084947) for fly stocks and P. Lasko, H. Steller, and R. Wharton for antibodies. This work was supported by the National Institutes of Health (F32 HD056779 to E.C.O and R01 GM061107 to E.R.G).

References

Abbott, M.K., Lengyel, J.A., 1991. Embryonic head involution and rotation of male terminalia require the *Drosophila* locus *head involution defective*. Genetics 129, 783–789.
Abdelwahid, E., Yokokura, T., Krieser, R.J., Balasundaram, S., Fowle, W.H., White, K., 2007. Mitochondrial disruption in Drosophila apoptosis. Dev. Cell 12, 793–806.
Aberle, H., Haghighi, A.P., Fetter, R.D., McCabe, B.D., Magalhães, T.R., Goodman, C.S., 2002. *Wishful thinking* encodes a BMP type II receptor that regulates synaptic growth in *Drosophila*. Neuron 33, 545–558.
Baines, R.A., 2005. Neuronal homeostasis through translational control. Mol. Neurobiol. 32, 113–121.
Bassell, G.J., Warren, S.T., 2008. Fragile X Syndrome: loss of local mRNA regulation alters synaptic development and function. Neuron 60, 201–214.
Bernstein, D., Hook, B., Hajarnavis, A., Opperman, L., Wickens, M., 2005. Binding specificity and mRNA targets of a *C. elegans* PUF protein, FBF-1. RNA 11, 447–458.
Brechbiel, J.L., Gavis, E.R., 2008. Spatial regulation of *nanos* is required for its function in dendrite morphogenesis. Curr. Biol. 18, 745–750.
Cho, P.F., Gamberi, C., Cho-Park, Y.A., Cho-Park, I.B., Lasko, P., Sonenberg, N., 2006. Cap-dependent translational inhibition establishes two opposing morphogen gradients in *Drosophila* embryos. Curr. Biol. 16, 2035–2041.
Clark, I.E., Dobi, K.C., Duchow, H.K., Vlasak, A.N., Gavis, E.R., 2002. A common translational control mechanism functions in axial patterning and neuroendocrine signaling in *Drosophila*. Development 129, 3325–3334.
Curtis, D., Treiber, D.K., Tao, F., Zamore, P.D., Williamson, J.R., Lehmann, R., 1997. A CCHC metal-binding domain in Nanos is essential for translational regulation. EMBO J. 16, 834–843.
Dietzl, G., Chen, D., Schnorrer, F., Su, K.C., Barinova, Y., Fellner, M., Gasser, B., Kinsey, K., Oppel, S., Scheiblauer, S., Couto, A., Marra, V., Keleman, K., Dickson, B.J., 2007. A genome-wide transgenic RNAi library for conditional gene inactivation in *Drosophila*. Nature 448, 151–156.
Eberwine, J., Miyashiro, K., Kacharmina, J.E., Job, C., 2001. Local translation of classes of mRNAs that are targeted to neuronal dendrites. Proc. Natl. Acad. Sci. U. S. A. 98, 7080–7085.
Edwards, T.A., Wilkinson, B.D., Wharton, R.P., Aggarwal, A.K., 2003. Model of the Brain Tumor-Pumilio translational repressor complex. Genes Dev. 17, 2508–2513.
Fallini, C., Zhang, H., Su, Y., Silani, V., Singer, R.H., Rossoll, W., Bassell, G.J., 2011. The survival of motor neuron (SMN) protein interacts with the mRNA-binding protein HuD and regulates localization of poly(A) mRNA in primary motor neuron axons. J. Neurosci. 31, 3914–3925.
Forbes, A., Lehmann, R., 1998. Nanos and Pumilio have critical roles in the development and function of *Drosophila* germline stem cells. Development 125, 679–690.
Frank, D.J., Edgar, B.A., Roth, M.B., 2002. The *Drosophila melanogaster* gene *brain tumor* negatively regulates cell growth and ribosomal RNA synthesis. Development 129, 399–407.
Grueber, W.B., Jan, L.Y., Jan, Y.N., 2003. Different levels of the homeodomain protein Cut regulate distinct dendrite branching patterns of *Drosophila* multidendritic neurons. Cell 112, 805–818.
Grueber, W.B., Ye, B., Yang, C.H., Younger, S., Borden, K., Jan, L.Y., Jan, Y.N., 2007. Projections of *Drosophila* multidendritic neurons in the central nervous system: links with peripheral dendrite morphology. Development 134, 55–64.
Haining, W.N., Carboy-Newcomb, C., Wei, C.L., Steller, H., 1999. The proapoptotic function of *Drosophila* Hid is conserved in mammalian cells. Proc. Natl. Acad. Sci. U. S. A. 96, 4936–4941.
Harris, R.E., Pargett, M., Sutcliffe, C., Umulis, D., Ashe, H.L., 2011. Brat promotes stem cell differentiation via control of a bistable switch that restricts BMP signaling. Dev. Cell 20, 72–83.
Jinushi-Nakao, S., Arvind, R., Amikura, R., Kinameri, E., Liu, A.W., Moore, A.W., 2007. Knot/Collier and Cut control different aspects of dendrite cytoskeleton and synergize to define final arbor shape. Neuron 56, 963–978.
Job, C., Eberwine, J., 2001. Localization and translation of mRNA in dendrites and axons. Nat. Rev. Neurosci. 2, 889–898.
Kuo, C.T., Zhu, S., Younger, S., Jan, L.Y., Jan, Y.N., 2006. Identification of E2/E3 ubiquitinating enzymes and caspase activity regulating *Drosophila* sensory neuron dendrite pruning. Neuron 51, 283–290.
Lee, T., Luo, L., 2001. Mosaic analysis with a repressible cell marker (MARCM) for *Drosophila* neural development. Trends Neurosci. 24, 251–254.
Lee, A., Li, W., Xu, K., Bogert, B.A., Su, K., Gao, F.B., 2003. Control of dendritic development by the *Drosophila* fragile X-related gene involves the small GTPase Rac1. Development 130, 5543–5552.
Li, W., Wang, F., Menut, L., Gao, F.B., 2004. BTB/POZ-zinc finger protein Abrupt suppresses dendritic branching in a neuronal subtype-specific and dosage-dependent manner. Neuron 43, 823–834.
Marek, K.W., Ng, N., Fetter, R., Smolik, S., Goodman, C.S., Davis, G.W., 2000. A genetic analysis of synaptic development: pre- and postsynaptic dCBP control transmitter release at the *Drosophila* NMJ. Neuron 25, 537–547.
Martin, K.C., 2004. Local protein synthesis during axon guidance and synaptic plasticity. Curr. Opin. Neurobiol. 14, 305–310.
Meijering, E., Jacob, M., Sarria, J.C.F., Steiner, P., Hirling, H., Unser, M., 2004. Design and validation of a tool for neurite tracing and analysis in fluorescence microscopy images. Cytometry A 58, 167–176.
Menon, K.P., Sanyal, S., Habara, Y., Sanchez, R., Wharton, R.P., Ramaswami, M., et al., 2004. The translational repressor Pumilio regulates presynaptic morphology and controls postsynaptic accumulation of translation factor eIF-4E. Neuron 44, 663–676.
Menon, K.P., Andrews, S., Murthy, M., Gavis, E.R., Zinn, K., 2009. The translational repressors Nanos and Pumilio have divergent effects on presynaptic terminal growth

and postsynaptic glutamate receptor subunit composition. J. Neurosci. 29, 5558–5572.
Mikl, M., Vendra, G., Doyle, M., Kiebler, M.A., 2010. RNA localization in neurite morphogenesis and synaptic regulation: current evidence and novel approaches. J. Comp. Physiol. 196, 321–334.
Muraro, N.I., Weston, A.J., Gerber, A.P., Luschnig, S., Moffat, K.G., Baines, R.A., 2008. Pumilio binds *para* mRNA and requires Nanos and Brat to regulate sodium current in *Drosophila* motoneurons. J. Neurosci. 28, 2099–2109.
Parisi, M., Lin, H., 2000. Translational repression: a duet of Nanos and Pumilio. Curr. Biol. 10, R81–R83.
Parrish, J.Z., Emoto, K., Kim, M.D., Jan, Y.N., 2007. Mechanisms that regulate establishment, maintenance, and remodeling of dendritic fields. Annu. Rev. Neurosci. 30, 399–423.
Parrish, J.Z., Xu, P., Kim, C.C., Jan, L.Y., Jan, Y.N., 2009. The microRNA *bantam* functions in epithelial cells to regulate scaling growth of dendrite arbors in *Drosophila* sensory neurons. Neuron 63, 788–802.
Ranganayakulu, G., Schulz, R.A., Olson, E.N., 1996. Wingless signaling induces *nautilus* expression in the ventral mesoderm of the *Drosophila* embryo. Dev. Biol. 176, 143–148.
Rees, J.S., Lowe, N., Armean, I.M., Roote, J., Johnson, G., Drummond, E., Spriggs, H., Ryder, E., Russell, S., St Johnston, D., Lilley, K.S., 2011. In vivo analysis of proteomes and interactomes using parallel affinity capture (iPAC) coupled to mass spectrometry. Mol. Cell. Proteomics 10 (M110.002386).
Rumpf, S., Lee, S.B., Jan, L.Y., Jan, Y.N., 2011. Neuronal remodeling and apoptosis require VCP-dependent degradation of the apoptosis inhibitor DIAP1. Development 138, 1153–1160.
Sato, K., Hayashi, Y., Ninomiya, Y., Shigenobu, S., Arita, K., Mukai, M., Kobayashi, S., 2007. Maternal Nanos represses *hid/skl*-dependent apoptosis to maintain the germ line in *Drosophila* embryos. Proc. Natl. Acad. Sci. U. S. A. 104, 7455–7460.
Schuman, E.M., Dynes, J.L., Steward, O., 2006. Synaptic regulation of translation of dendritic mRNAs. J. Neurosci. 26, 7143–7146.
Shukla, A., Tapadia, M.G., 2011. Differential localization and processing of apoptotic proteins in Malpighian tubules of *Drosophila* during metamorphosis. Eur. J. Cell Biol. 90, 72–80.
Sonoda, J., Wharton, R.P., 2001. *Drosophila* Brain Tumor is a translational repressor. Genes Dev. 15, 762–773.
Tao, J., Rolls, M.M., 2011. Dendrites have a rapid program of injury-induced degeneration that is molecularly distinct from developmental pruning. J. Neurosci. 31, 5398–5405.
Thompson, B., Wickens, M., Kimble, J., 2007. Translational control in development. In: Mathews, M.B., Sonenberg, N., Hershey, J.W.B. (Eds.), Translational Control in Biology and Medicine. Cold Spring Harbor Laboratory Press, NY, pp. 507–544.
Williams, D.W., Truman, J.W., 2005a. Cellular mechanisms of dendrite pruning in *Drosophila*: insights from in vivo time-lapse of remodeling dendritic arborizing sensory neurons. Development 132, 3631–3642.
Williams, D.W., Truman, J.W., 2005b. Remodeling dendrites during insect metamorphosis. J. Neurobiol. 64, 24–33.
Williams, D.W., Kondo, S., Krzyzanowska, A., Hiromi, Y., Truman, J.W., 2006. Local caspase activity directs engulfment of dendrites during pruning. Nat. Neurosci. 9, 1234–1236.
Wu, C.W., Zeng, F., Eberwine, J., 2007. mRNA transport to and translation in neuronal dendrites. Anal. Bioanal. Chem. 387, 59–62.
Ye, B., Petritsch, C., Clark, I.E., Gavis, E.R., Jan, L.Y., Jan, Y.N., 2004. Nanos and Pumilio are essential for dendrite morphogenesis in *Drosophila* peripheral neurons. Curr. Biol. 14, 314–321.